Title

Chemical shift assignments of the C-terminal domain of CaBP1 bound to the IQ-motif of voltage-gated Ca2+ channel (CaV1.2)

Journal

Biomolecular NMR Assignments, 16(2)

ISSN

1874-2718

Authors

Salveson, Ian
Ames, James B

Publication Date

2022-10-01

DOI

10.1007/s12104-022-10108-0

Peer reviewed

Biomolecular NMR Assignments (2022) 16:385–390
https://doi.org/10.1007/s12104-022-10108-0

ARTICLE

Chemical shift assignments of the C-terminal domain of CaBP1 bound to the IQ-motif of voltage-gated Ca^{2+} channel ($Ca_V1.2$)

Ian Salveson[1] · James B. Ames[1]

Received: 2 August 2022 / Accepted: 31 August 2022 / Published online: 5 September 2022

Abstract

The neuronal L-type voltage-gated Ca^{2+} channel ($Ca_V1.2$) interacts with Ca^{2+} binding protein 1 (CaBP1), that promotes Ca^{2+}-induced channel activity. The binding of CaBP1 to the IQ-motif in $Ca_V1.2$ (residues 1644–1665) blocks the binding of calmodulin and prevents Ca^{2+}-dependent inactivation of $Ca_V1.2$. This Ca^{2+}-induced binding of CaBP1 to $Ca_V1.2$ is important for modulating neuronal synaptic plasticity, which may serve a role in learning and memory. Here we report NMR assignments of the C-terminal domain of CaBP1 (residues 99–167, called CaBP1C) that contains two Ca^{2+} bound at the third and fourth EF-hands (EF3 and EF4) and is bound to the $Ca_V1.2$ IQ-motif from $Ca_V1.2$ (BMRB accession no. 51518).

Keywords CaBP1 · EF-hand · $Ca_V1.2$ · IQ-motif · Calmodulin · CDI

Biological context

$Ca_V1.2$ controls the excitability of the postsynaptic membrane in hippocampal neurons, which is important for learning and memory (Hell et al. 1993; Moosmang et al. 2005; Vogl et al. 2015). The cytosolic C-terminal region of $Ca_V1.2$ (residues 1644–1665, called IQ-motif) is important for promoting Ca^{2+}-dependent inactivation (CDI) of $Ca_V1.2$ (Erickson et al. 2001; Zuhlke et al. 1999). Ca^{2+}-free CaM has been suggested to bind to the IQ-motif to increase the channel open probability under basal conditions (Adams et al. 2014; Erickson et al. 2001). $Ca_V1.2$ channel opening promotes a rise in intracellular Ca^{2+} sensed by CaM that causes a Ca^{2+}-induced conformational change in the CaM/$Ca_V1.2$ complex leading to CDI (Ben Johny et al. 2013; Peterson et al. 1999; Zuhlke et al. 1999). CaBP1 competes with CaM for binding to the IQ-motif (Findeisen et al. 2013; Hardie and Lee 2016), which prevents channel pre-association of CaM and abolishes CDI (Hardie and Lee 2016; Oz et al. 2011). Thus, CaBP1 serves as a competitive inhibitor of CDI and promotes constitutive channel activation at high Ca^{2+} levels (Hardie and Lee 2016; Oz et al. 2011), in contrast to CaM that causes Ca^{2+}-induced channel inactivation (Peterson et al. 1999; Zuhlke et al. 1999). In essence, CaBP1 and CaM oppositely regulate $Ca_V1.2$ channel activity by serving as an accelerator and brake, respectively (Ames 2021). We report NMR resonance assignments for the C-terminal domain of CaBP1 (CaBP1C) with two Ca^{2+} bound that is bound to the IQ-motif of $Ca_V1.2$ (called CaBP1C-IQ) as a first step toward elucidating the intermolecular contacts between CaBP1 and $Ca_V1.2$.

Methods and experiments

Preparation of CaBP1C bound to the $Ca_V1.2$ IQ-motif

A cDNA of *Homo sapiens* CaBP1C was subcloned into pET-11b vector (Novagen) that produced recombinant CaBP1C without any extra residues. Recombinant CaBP1C uniformly labeled with ^{13}C and ^{15}N was expressed in bacterial cells grown on M9 minimal media supplemented with ^{15}N-labeled NH_4Cl (1 g per liter of cell culture) and ^{13}C-labeled glucose (3 g per liter). The isotopically labeled CaBP1C was purified as described previously (Li et al. 2009). A peptide representing the $Ca_V1.2$ IQ-motif (residues 1642–1665) was purchased from GenScript, dissolved in DMSO-d_6 and quantified using UV–Vis absorption. A 2.0-fold excess of IQ peptide was added to Ca^{2+}-bound CaBP1C and the complex was concentrated to 500 µM in the presence of 2 mM $CaCl_2$ using a 3 K Amicon concentrator.

✉ James B. Ames
jbames@ucdavis.edu

[1] Department of Chemistry, University of California, Davis, Davis, CA 95616, USA

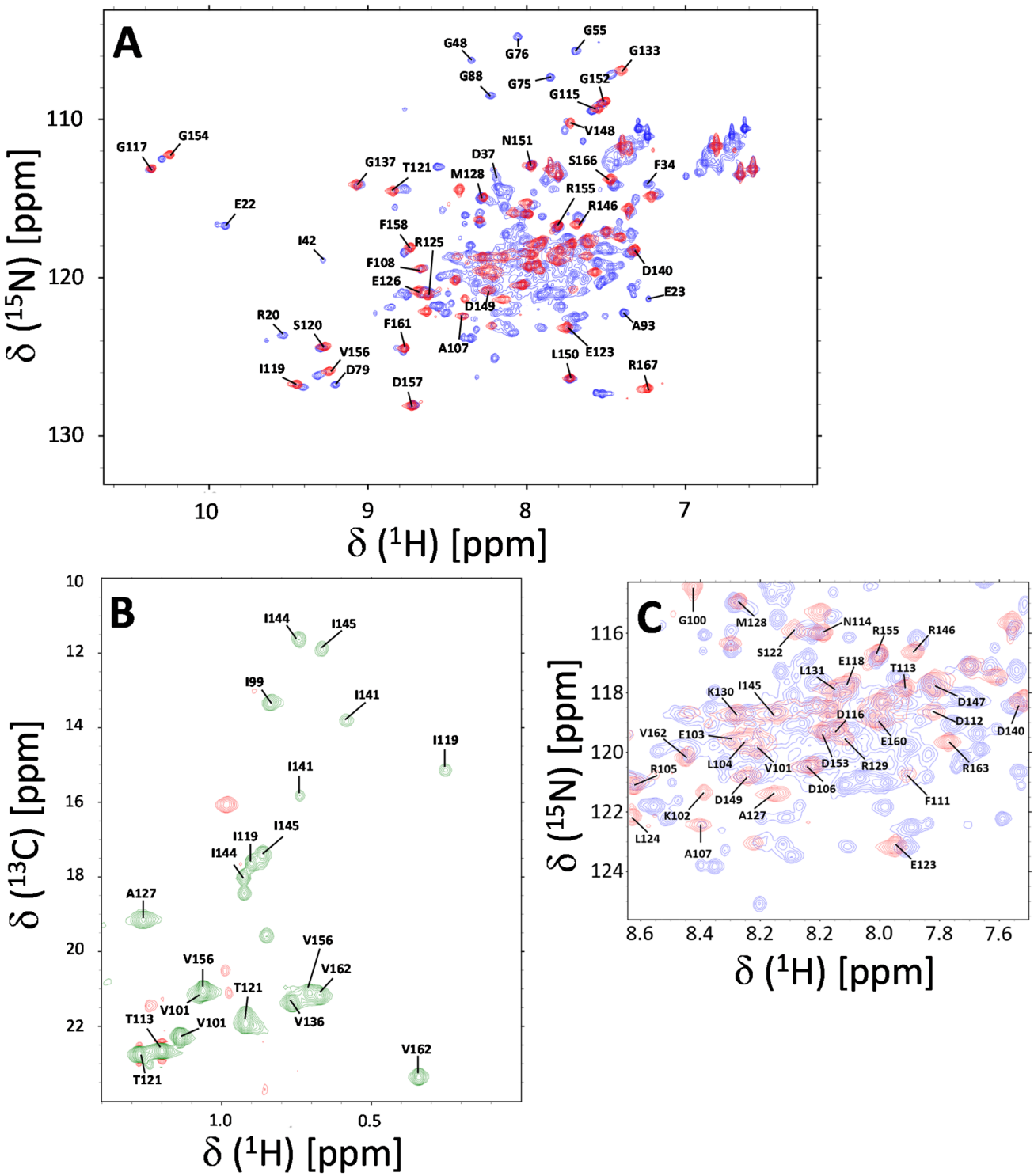

Fig. 1 **A** Two-dimensional ^{15}N-^{1}H HSQC NMR spectrum of ^{15}N-labeled full-length CaBP1 (blue) and CaBP1C (red) both bound to unlabeled $Ca_V1.2$ IQ peptide at pH 7.5 recorded at 600-MHz ^{1}H frequency. **B** Constant-time ^{13}C-^{1}H HSQC spectrum of ^{13}C-labeled CaBP1C bound to unlabeled IQ peptide. **C** Expanded view of the spectrally crowded region from panel **A**. Representative assignments are indicated by the labeled peaks; complete assignments are available as BMRB accession no. 51518

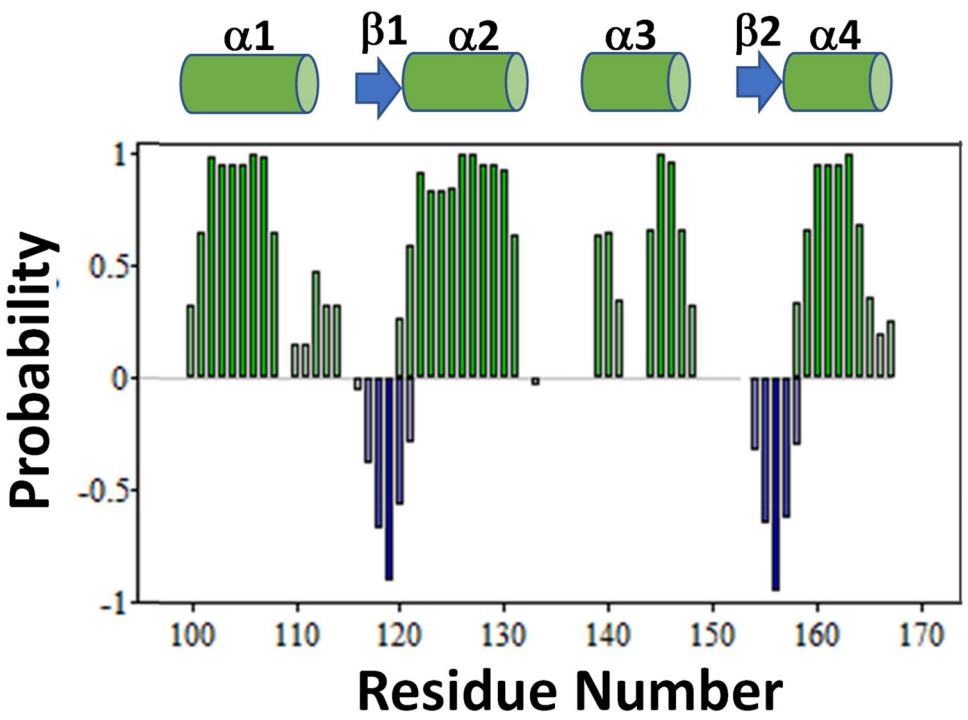

Fig. 2 Secondary structure of CaBP1C bound to $Ca_V1.2$ IQ. TALOS ANN-secondary structure probability plotted as a function of residue number. Secondary structure elements are represented as green cylinders (helix) and blue arrows (β-strand)

NMR spectroscopy

Samples of CaBP1C-IQ for NMR were prepared by exchanging the complex into a buffer containing 20 mM Tris-d_{11} (pH 7.5) with 2 mM $CaCl_2$, and 92% H_2O/8% D_2O. All NMR experiments were performed at 308 K on a Bruker Avance 600 MHz spectrometer equipped with a four-channel interface and triple resonance cryogenic (TCI) probe. The ^{15}N-^{1}H HSQC spectrum (Fig. 1) contained 256 × 2048 complex points for ^{15}N(F1) and ^{1}H(F2), respectively. Backbone resonances were assigned by analyzing HNCA, HNCACB, CBCA(CO)NH, HNCO (Ikura et al. 1990). Side chain resonances were assigned by analyzing HCCCONH-TOCSY, HCCH-TOCSY as described previously (Ikura et al. 1991). The NMR data were processed using NMRFx Analyst (Norris et al. 2016) and analyzed using Sparky NMRFAM (Lee et al. 2015).

Extent of assignments and data deposition

Ideally, we would want to perform NMR structural analysis of the full-length CaBP1 bound to the $Ca_V1.2$ IQ. Unfortunately, the full-length CaBP1 forms a dimer and other oligomeric species at the protein concentrations required for 3D NMR, and the relatively large size of the protein dimer reduces the sensitivity of the triple resonance 3D NMR experiments. Instead, we chose to perform NMR structural analysis of the C-terminal domain of CaBP1 (residues 99–167, called CaBP1C) that is monomeric in solution (Li et al. 2009) and exhibits functional binding to the IQ peptide (Fig. 1A). A two-dimensional ^{15}N-^{1}H HSQC NMR spectrum of full-length CaBP1 bound to the IQ peptide (at 0.05 mM protein concentration where CaBP1-IQ is monomeric) demonstrates that the chemical shifts of the CaBP1 C-terminal domain are similar to those of CaBP1C bound to the IQ (Fig. 1A, C). The chemical shifts of the C-terminal domain residues of CaBP1 bound to the IQ are quite different from those of CaBP1 in the absence of the IQ, demonstrating that the IQ peptide binds to the CaBP1 C-terminal domain (Wingard et al. 2005). Also, the chemical shifts of the N-terminal domain residues of CaBP1 bound to the IQ (Fig. 1A) are the same (within experimental error) as those of CaBP1 in the absence of the IQ (Wingard et al. 2005). These results demonstrate that the IQ peptide binds solely to the C-terminal domain of CaBP1 (without contacting the N-terminal domain), and IQ binding to CaBP1C is structurally similar to that of full-length CaBP1.

The two-dimensional ^{15}N-^{1}H HSQC NMR spectrum of ^{15}N-labeled CaBP1C bound to unlabeled $Ca_V1.2$ IQ peptide (called CaBP1C-IQ) illustrates representative NMR assignments (labeled red peaks in Fig. 1A). NMR assignments were derived from triple resonance NMR experiments performed on ^{13}C/^{15}N-labeled CaBP1C bound to unlabeled IQ peptide. The high level of chemical shift dispersion indicates that CaBP1C-IQ complex is stably folded. The large downfield chemical shifts of the amide resonances assigned to G117 and G154 confirm that Ca^{2+}

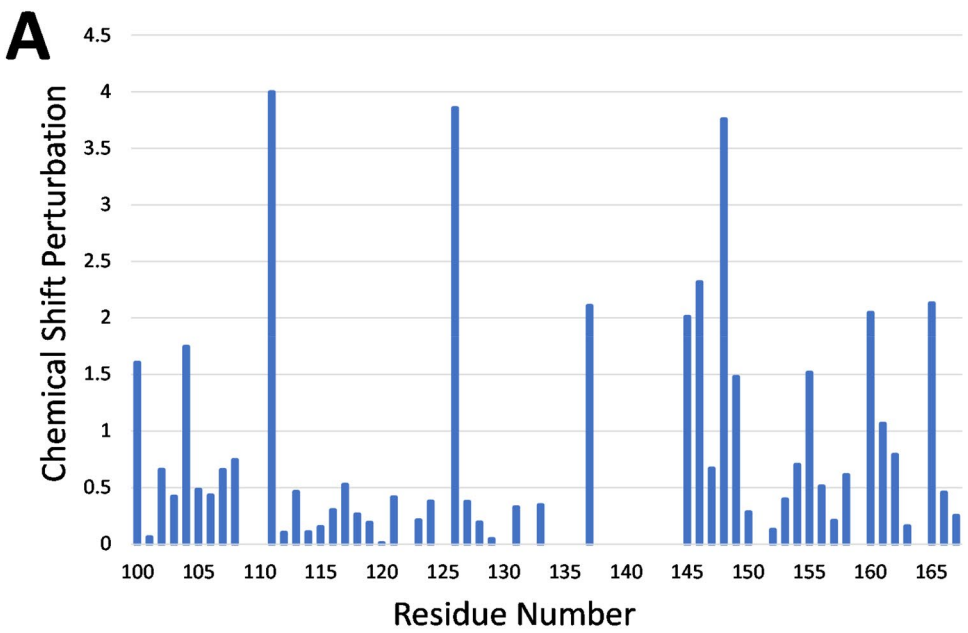

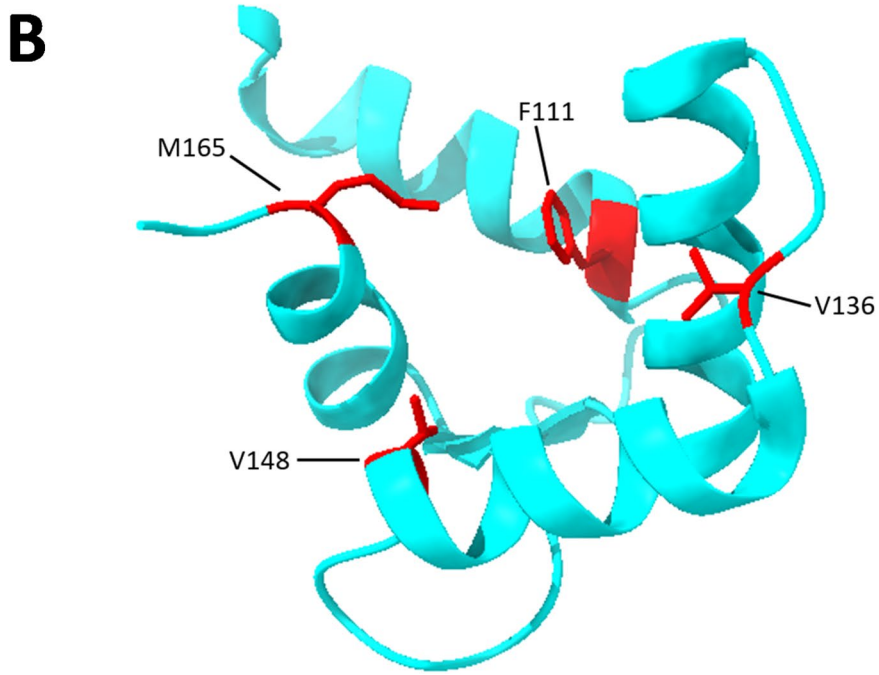

Fig. 3 **A** Amide chemical shift perturbation for CaBP1C caused by the binding of IQ peptide. Chemical shift perturbation (CSP) was calculated as $CSP = \{(HN_A - HN_B)^2 + (^{15}N_A - ^{15}N_B)^2\}^{1/2}$. HN_A and HN_B are HN chemical shift of CaBP1C in the presence versus absence of IQ peptide, and $^{15}N_A$ and $^{15}N_B$ are ^{15}N chemical shift of CaBP1C in the presence versus absence of IQ peptide. Chemical shifts of CaBP1C (in the absence of IQ) were obtained from BMRB 15623. **B** Crystal structure of the C-terminal domain of CaBP1 (Findeisen and Minor 2010). Exposed hydrophobic residues with the largest chemical shift perturbation are highlighted in red

is bound to EF3 and EF4 in CaBP1C (Fig. 1A). Other noteworthy downfield shifts were assigned to I119, S120 and V156 that are located in the EF-hand β-strands and are predicted to form antiparallel β-sheets with strong backbone amide hydrogen bonds. The upfield-shifted chemical shifts of methyl resonances assigned to residues I119, I141 and V162 (Fig. 1B) suggest that these residues may be located in the hydrophobic core near aromatic residues. More than 87% of the main chain ^{13}C resonances ($^{13}C\alpha$, $^{13}C\beta$, and ^{13}CO), 85% of backbone amide resonances (^{1}HN, ^{15}N), and 74% of methyl side chain resonances were assigned. Side chain aromatic resonances from F108, F111, F158, and F161 appear exchange broadened in the NMR spectra and could not be assigned. The unassigned amide resonances from non-proline residues (110, 122, 125, 132, 134, 138, 139, 140, 141, 142, 143, 159, 164) had weak or missing NMR intensities that prevented their assignment. In particular, a stretch of residues between

EF3 and EF4 (residues 138–143) could not be assigned due to weak NMR intensities, perhaps because this linker region is conformationally disordered or otherwise unstructured. A complete list of the chemical shift assignments (^{1}H, ^{15}N, ^{13}C) of CaBP1C-IQ have been deposited in the BioMagResBank under accession number 51518.

The secondary structure of CaBP1C bound to the IQ peptide was calculated on the basis of chemical shift index (Wishart et al. 1992) and ANN-secondary structure prediction using TALOS (Shen et al. 2009) (Fig. 2). As expected, CaBP1C-IQ contains two EF-hands with four α-helices: α1 (residues 101–110), α2 (residues 121–132), α3 (residues 140–148) and α4 (residues 158–165) shown as green cylinders in Fig. 2. Conserved β-strands were observed in EF3 (residues 118–120, β1) and EF4 (residues 155–157, β2) shown as blue arrows in Fig. 2. The overall secondary structure of CaBP1C-IQ is similar to that of the crystal structure of CaBP1 (Findeisen and Minor 2010). A plot of the amide chemical shift perturbation caused by the binding of the IQ peptide reveals that CaBP1C residues F111, E126, V136, R146, V148, E160 and M165 exhibit the largest CSP values (Fig. 3A). Hydrophobic residues F111, V136, V148 and M165 are located in an exposed cleft in the crystal structure that are likely making intermolecular hydrophobic contacts with the IQ peptide (Fig. 3B). The NMR assignments of CaBP1C bound to the $Ca_V1.2$ IQ-motif are a first step toward determining the three-dimensional structure of CaBP1 bound to $Ca_V1.2$.

Acknowledgements We thank Derrick Kaseman and Ping Yu for technical support and help with NMR experiments performed at the UC Davis NMR Facility.

Author contributions IS performed all experiments, analyzed data and helped write the manuscript. JBA directed the overall project and wrote the manuscript.

Funding Work supported by NIH grants to J.B.A (R01 GM130925) and to the UC Davis NMR Facility (RR11973).

Data availability The assignments have been deposited to the BMRB under the accession code: 51518.

Declarations

Conflict of interest The authors declare they have no competing conflict of interest.

Ethical approval The experiments comply with the current laws of the United States.

References

Adams PJ, Ben-Johny M, Dick IE, Inoue T, Yue DT (2014) Apocalmodulin itself promotes ion channel opening and Ca(2+) regulation. Cell 159:608–622

Ames JB (2021) L-type Ca(2+) channel regulation by calmodulin and CaBP1. Biomolecules 11:1811

Ben Johny M, Yang PS, Bazzazi H, Yue DT (2013) Dynamic switching of calmodulin interactions underlies Ca2+ regulation of CaV.13 channels. Nat Commun 4:1717

Erickson M, Alseikhan B, Peterson B, Yue D (2001) Preassociation of calmodulin with voltage-gated Ca(2+) channels revealed by FRET in single living cells. Neuron 31:973–985

Findeisen F, Minor DL (2010) Structural basis for the differential effects of CaBP1 and calmodulin on CaV1.2 calcium-dependent inactivation. Structure 18:1617–1631

Findeisen F, Rumpf CH, Minor DL Jr (2013) Apo states of calmodulin and CaBP1 control CaV1 voltage-gated calcium channel function through direct competition for the IQ domain. J Mol Biol 425:3217–3234

Hardie J, Lee A (2016) Decalmodulation of Cav1 channels by CaBPs. Channels 10:33–37

Hell JW, Westenbroek RE, Warner C, Ahlijanian MK, Prystay W, Gilbert MM, Snutch TP, Catterall WA (1993) Identification and differential subcellular localization of the neuronal class C and class D L-type calcium channel alpha 1 subunits. J Cell Biol 123:949–962

Ikura M, Kay LE, Bax A (1990) A novel approach for sequential assignment of 1H, 13C, and 15N spectra of proteins: heteronuclear triple-resonance three-dimensional NMR spectroscopy. Appl Calmodulin Biochem 29:4659–4667

Ikura M, Spera S, Barbato G, Kay LE, Krinks M, Bax A (1991) Secondary structure and side-chain 1H and 13C resonance assignments of calmodulin in solution by heteronuclear multidimensional NMR spectroscopy. Biochemistry 30:9216–9228

Lee W, Tonelli M, Markley JL (2015) NMRFAM-SPARKY: enhanced software for biomolecular NMR spectroscopy. Bioinformatics 31:1325–1327

Li C, Chan J, Haeseleer F, Mikoshiba K, Palczewski K, Ikura M, Ames JB (2009) Structural insights into Ca2+-dependent regulation of inositol 1,4,5-trisphosphate receptors by CaBP1. J Biol Chem 284:2472–2481

Moosmang S, Haider N, Klugbauer N, Adelsberger H, Langwieser N, Muller J, Stiess M, Marais E, Schulla V, Lacinova L, Goebbels S, Nave K, Storm D, Hofmann F, Kleppisch T (2005) Role of hippocampal Cav1.2 Ca2+ channels in NMDA receptor-independent synaptic plasticity and spatial memory. J Neurosci 25:9883–9892

Norris M, Fetler B, Marchant J, Johnson BA (2016) NMRFx Processor: a cross-platform NMR data processing program. J Biomol NMR 65:205–216

Oz S, Tsemakhovich V, Christel CJ, Lee A, Dascal N (2011) CaBP1 regulates voltage-dependent inactivation and

activation of Ca(V)1.2 (L-type) calcium channels. J Biol Chem 286:13945–13953

Peterson B, DeMaria C, Adelman J, Yue D (1999) Calmodulin is the Ca2+ sensor for Ca2+ -dependent inactivation of L-type calcium channels. Nature 22:549–558

Shen Y, Delaglio F, Cornilescu G, Bax A (2009) TALOS+: a hybrid method for predicting protein backbone torsion angles from NMR chemical shifts. J Biomol NMR 44:213–223

Vogl AM, Brockmann MM, Giusti SA, Maccarrone G, Vercelli CA, Bauder CA, Richter JS, Roselli F, Hafner AS, Dedic N, Wotjak CT, Vogt-Weisenhorn DM, Choquet D, Turck CW, Stein V, Deussing JM, Refojo D (2015) Neddylation inhibition impairs spine development, destabilizes synapses and deteriorates cognition. Nat Neurosci 18:239–251

Wingard JN, Chan J, Bosanac I, Haeseleer F, Palczewski K, Ikura M, Ames JB (2005) Structural analysis of Mg2+ and Ca2+ binding to CaBP1, a neuron-specific regulator of calcium channels. J Biol Chem 280:37461–37470

Wishart DS, Sykes BD, Richards FM (1992) The chemical shift index: a fast and simple method for the assignment of protein secondary structure through NMR spectroscopy. Biochemistry 31:1647–1651

Zuhlke RD, Pitt GS, Deisseroth K, Tsien RW, Reuter H (1999) Calmodulin supports both inactivation and facilitation of L-type calcium channels. Nature 399:159–162